The impact of curcumin derived polyphenols on the structure and flexibility COVID-19 main protease binding pocket: a molecular dynamics simulation study

Aweke Mulu[1], Mulugeta Gajaa[2], Haregewoin Bezu Woldekidan[1] and Jerusalem Fekadu W/mariam[1]

[1] College of Applied Science, Addis Ababa Science and Technology University, Addis Ababa, Ethiopia
[2] College of Natural and Social science, Addis Ababa Science and Technology University, Addis Ababa, Ethiopia

ABSTRACT

The newly occurred SARS-CoV-2 caused a leading pandemic of coronavirus disease (COVID-19). Up to now it has infected more than one hundred sixty million and killed more than three million people according to 14 May 2021 World Health Organization report. So far, different types of studies have been conducted to develop an anti-viral drug for COVID-19 with no success yet. As part of this, silico were studied to discover and introduce COVID-19 antiviral drugs and results showed that protease inhibitors could be very effective in controlling. This study aims to investigate the binding affinity of three curcumin derived polyphenols against COVID-19 the main protease (Mpro), binding pocket, and identification of important residues for interaction. In this study, molecular modeling, auto-dock coupled with molecular dynamics simulations were performed to analyze the conformational, and stability of COVID-19 binding pocket with diferuloylmethane, demethoxycurcumin, and bisdemethoxycurcumin. All three compounds have shown binding affinity −39, −89 and −169.7, respectively. Demethoxycurcumin and bisdemethoxycurcumin showed an optimum binding affinity with target molecule and these could be one of potential ligands for COVID-19 therapy. And also, COVID-19 main protease binding pocket binds with the interface region by one hydrogen bond. Moreover, the MD simulation parameters indicated that demethoxycurcumin and bisdemethoxycurcumin were stable during the simulation run. These findings can be used as a baseline to develop therapeutics with curcumin derived polyphenols against COVID-19.

Subjects Biophysics, Computational Biology, Molecular Biology, Pharmacology, Computational Science
Keywords NAMD, X-ray crustal structure, SARS-CoV-2, Docking, Binding energy

INTRODUCTION

The severe acute respiratory syndrome coronavirus 2 (SARS-CoV-2), which was first reported in Hubei Province of Wuhan, China in December 2019, is responsible for the ongoing global pandemic of coronavirus disease 2019 (COVID-19) spreading across almost all countries with 160,686,749 active infection cases and 3,335,948 deaths until

14 May 2021 (*World Health Organization, 2020*; *Guarner, 2020*; *WHO, 2020*). The actual number of cases presumed much higher, due to limitations in testing, lack of medication, and applying World Health Organization recommendations such as social distancing, hand washing, and travel ban and full lockdown in many cities (*World Health Organization, 2020*; *Chen, Liu & Guo, 2020*; *WHO, 2020*). Prior work in this area showed that SARS-CoV-2 is the third coronavirus belonging to Genus Beta coronavirus that can infect human next coronavirus-severe acute respiratory syndrome (SARS-CoV-2) and the Middle East respiratory syndrome (MERS-CoV) (*Guarner, 2020*). SARS-CoV-2, the virus responsible for COVID-19, belongs to a group of genetically-related viruses that includes SARS-COV and some other CoVs isolated from bat populations (*World Health Organization, 2020*). The SARS-CoV-2 virus is the primary causative agent of COVID-19. The pol gene of the SARS-CoV-2 virus possesses a positive-sense ~30 kb long RNA genome with ~14 ORFs and encoding 27 proteins (*Chen, Liu & Guo, 2020*; *Hoque et al., 2020*). Among multiple encoded proteins programmed ribosomal frameshifting generates two polyproteins encoding the replicase proteins (*Zhao, Weber & Yang, 2013*). The range of viral processing protein associated with structural proteins, non-structural proteins, and accessory proteins have been reported in several studies (*World Health Organization, 2020*; *Zhao, Weber & Yang, 2013*; *Pal et al., 2020*). The pol gene of the SARS-CoV-2 virus encodes two protease enzymes main protease (Mpro) and Papain-like protease, which are involved in the proteolytic processing of the polyproteins into individual nsp7/nsp8/nsp12 to control viral gene expression and replication in the host (*Chen, Liu & Guo, 2020*; *Zhao, Weber & Yang, 2013*; *Pal et al., 2020*). SARS-CoV-2 virus Mpro is a vital enzyme that catalyzes the proteolytic process, non-structural proteins (nsps) generated by the main protease play a major role in the reverse-transcribed viral DNA into the host genome (*Zhao, Weber & Yang, 2013*; *Woo et al., 2010*; *Elaswad et al., 2020*; *Parlikar et al., 2020*). It is composed of three structurally and functionally distinct domains I, II, and III. Domain I and II contain highly conserved Cys145-His41 residues located in the cleft which are directly involved in the catalytic activities of Mpro (*Jin et al., 2020*). Therefore, SARS-CoV-2 virus Mpro has emerged as a promising antiviral target as this is responsible for newly synthesized double-stranded viral DNA and subsequent maturation of polyproteins into host genomic DNA. SARS-CoV-2 virus Mpro inhibitors repurposing, which target the enzyme active site, have been studied computationally over the past few months to control COVID-19 as there is an urgent requirement for a strong drug or combination of drugs to combat the pandemic (*Muralidharan et al., 2020*; *Liu et al., 2020*). Currently, natural products are screened by molecular docking and molecular dynamic simulation to test their affinity towards molecular targets of COVID-19 taking the advantage that natural products are free from toxic or side effects (*Elaswad et al., 2020*; *Emran et al., 2015*; *Dash et al., 2014*). In this study, the structure of SARS-CoV-2 virus Mpro was obtained from the protein data bank (PDB) gave a major advance for structure-based drug design of Curcumin derivative polyphenols, and gives well-established techniques to reveal important dynamic information in proteins. This is an exciting new approach to develop effective therapies to fight COVID-19 with Curcumin, exploiting a new mechanism based on well-validated virulence factors. And also, expanding the list of lead compounds means more

possible drugs that could be advanced through clinical trials and better treatments will be possible shortly.

Up to now, there are no robust drugs for the widespread SARS-CoV-2 virus although there are now several vaccines that are in use. Finding a new drug in a wet lab and bringing it to market is hard, expensive, and time-consuming. Due to rapid ongoing global health emergency in the current outbreak and high mortality rate estimated by World Health Organization, the more rapid development of new antiviral drugs is highly demanded (*WHO, 2020*; *Hoque et al., 2020*). In the literature, traditional medicines have been extensively investigated to find novel therapeutic strategies for viruses including SARS-CoV-2. Evidence from several computational studies indicated that natural compounds for virus infection treatment play a critical role. A review of the literature showed that natural compounds with low cytotoxicity and high bioavailability seem to be the most efficient candidate's therapy. Also, studies observed lining modern medicine, humans have relayed to the use of phytochemicals for the treatment of different diseases (*Islam, Khan & Mishra, 2019*; *Forni et al., 2019*). In general, work to date in this area supports phytochemicals such as polyphenols possessing a variety of potential biological benefits such as anti-oxidant, anti-inflammatory, antiviral, and antibacterial benefits (*Hatcher et al., 2008*; *Anbarasu & Jayanthi, 2018*). A systematic review of peer-reviewed literature showed that Curcumin has antiviral activity in human immunodeficiency virus, herpes simplex virus, dengue virus, Zika, and chikungunya viruses (*Hatcher et al., 2008*; *Anbarasu & Jayanthi, 2018*; *Mounce et al., 2017*; *Praditya et al., 2019a*). The main objective of this work is to investigate methods for improving Curcumin derivative polyphenols that will be required for developing Mpro inhibitors were performed with silico study that included molecular docking combined with molecular dynamic simulation depend on Mpro binding pocket (PDB ID: 7BUY) (*Jin et al., 2020*). Specifically, we aim to investigate the amino acids that contribute the most to the binding Curcumin-derived polyphenols; we examined the binding mode of the Mpro pocket and found that form hydrogen bonds with binding pocket of residues. Finally, we put into MD simulation and binding free energy calculation. Results revealed that demethoxycurcumin and bisdemethoxycurcumin (especially bisdemethoxycurcumin) could have good inhibitory activity towards Mpro.

MATERIALS & METHODS

Protein and polyphenols structure preparation

The crystal structure of the MPro: carmofur complex (PDB ID: 7BUY) (*Jin et al., 2020*) was retrieved from the Protein Data Bank (PDB). A high-quality homology model of Apo-enzyme (without carmofur) was calculated using MODELLER version 9.10 (*Vanommeslaeghe, Raman & MacKerell, 2012*). Before docking, crystallographic water molecules and bound ligands were removed from 3D structures. The protonation states of acidic and basic residues were determined under pH 7.0 conditions and analyzed by the H++ server (*Anandakrishnan, Aguilar & Onufriev, 2012*). Next, the Modell structure was subjected to Discovery studio for optimization and minimization. Finally, validate the modeled structure using the UCLA-DOE server (http://servicesn.mbi.ucla.edu/)

(*Benkert, Künzli & Schwede, 2009*; *Colovos & Yeates, 1993*; *Pontius, Richelle & Wodak, 1996*). The modeled 3D structure was then validated and confirmed by using the RAMPAGE, ERRAT, and Verify3D online servers. After validating the homology models, we resolved the issue of mismatched residue and missed structure across the two models. The SMILES of the three natural polyphenols diferuloylmethane, demethoxycurcumin, and bisdemethoxycurcumin were obtained from Pub Chem (*Bolton et al., 2008*) and their accession numbers are DB969516, DB5469424, and DB5315472, respectively. These SMILES were converted to PDB format with 3 D coordinates using Open Babel (*O'Boyle et al., 2011*), an open-source chemical toolbox for the inter-conversion of chemical structures.

Docking methodology

The experiments were performed with Auto-Dock 4.2 according to the previous study procedure (*Morris et al., 2009*). The work was separated into two parts; the first was prepared ligand and protein pdbqt file and Docking Parameter file using Auto-Dock 4.2. The second was performed molecular docking and finally, the results were analyzed. Fourteen refined 3D polyphenols structures were screened for binding affinity and selectivity toward protein. To cover the whole protein structure global docking was conducted with the spacing of 0.5 Å. Subsequently, rigid or flexible docking of the target was performed and then the complexes with the lowest binding energies are selected. The genetic algorithm was used to evaluate parameters with the default setting, and Lamarckian GA (4.2) was employed for docking simulations. All docking parameters procedures were set to 150 genetic algorithm runs using the Lamarckian genetic algorithm conformational search, with the population size of 300, 2,500,000 maximum numbers of energy evaluations, and 27,000 generations per run. The best protein-polyphenols complexes were selected according to the molecular docking results including binding energy, root mean square deviation, and type of favorable interactions and binding sites.

Set simulation parameters and molecular dynamics

To explore the conformational flexibility of best hit compounds against free protein, an MD simulation study was employed using NAMD 2.3 tool on the Windows Operating System (*Nelson et al., 1996*). Each complex was separated for generating topology and coordinates. The protein topology and coordinate files were lacking in the Amber force field prepared by the general amber force field (CgenFF) Server (*Vanommeslaeghe, Raman & MacKerell, 2012*), while the ligands topology and coordinate files were generated using Open Babel (*O'Boyle et al., 2011*). The generated NAMD compatible files for the proteins and the ligands were then merged, and then complex subjected to solvated, minimized, and equilibrated. The systems were solvated in a cubic water-box with the explicit solvation model TIP3P.20 we used a distance of 1.0 Å between the cell wall and the solvated atoms of the system. Counter-ions were also added to neutralize the system. The energy minimization (n steps = 5,000) was conducted using the steepest descent approach (1,000 ps) for each protein-ligand complex. Particle Mesh Ewald (PME) method was employed for energy calculation and electrostatic and Van der Waals interactions;

cut-off distance for the short-range Van der Waals was set to 10 Å, where Coulomb cut-off and neighbor list were fixed at 8 Å. Finally, a 50 ns molecular dynamics simulation was carried out for all the complexes with n steps 1,000,000. The RMSD, hydrogen bond distribution, and RMSF analysis were carried out using MS Excel (2016), VMD, and UCSF Chimera 1.10.1 software. Trajectory snapshots were stored at every 0.2 ps during the simulation period, and 3D coordinate files were harvested after every 2 fs for post-dynamic analysis.

MM-PBSA approach Interaction energy

The binding energy of Mpro-Curcumin derivative polyphenols complexes was calculated using the molecular mechanics Poisson–Boltzmann surface area (MM-PBSA) method (*Kumari, Kumari & Lynn, 2014*). Free energy of solvation (TP3 solvent model) and molecular mechanics potential energy was calculated. In this study, snapshots were taken from MD simulation used for calculating binding free energy. The individual contributions of protein residues to the three energetic components were determined through per-residue decomposition. The temperature used for Poisson–Boltzmann calculation was set to 300 K.

Prediction of ADME by computational analysis

ADME analysis of Bisdemethoxycurcumin, Demethoxycurcumin, and Diferuloylmethane at pH 7 was examined using online software tools (*Baell & Holloway, 2012*). The important parameters related to ADME properties such as Proudfoot's rule of five, pharmacokinetic properties, drug likeliness, molar refractivity, and solubility of the drug was deliberated (*Daina, Michielin & Zoete, 2017*).

DISCUSSION

Until now, no specific antiviral medication was discovered for COVID-19 the only control measure includes proper hand washing, social distancing, mouth and nose masking, travel restriction, and infected person isolation (*World Health Organization, 2020*; *Guarner, 2020*; *Zhao, Weber & Yang, 2013*). Furthermore, Scientists around the world are developing many potential vaccines for COVID-19 and the biggest vaccination campaign in history is underway. However, according to the world meter report, the coronavirus COVID-19 is still affecting 219 countries and worldwide 160,686,749 people infected and 3,335,948 people died until May 14, 2021, 20:04 GMT. In the context of Ethiopia, this virus died about 3,951 people and infected 264,960 people. Viruses continually change through mutations and the gene encoding the S protein of SARS-CoV-2, various mutations have been reported and recently, the United Kingdom (UK) (VOC-202012/01 or VUI-202012/01 or B.1.1.7), Indian (B.1.617), and South Africa (501Y.V2 or 20C/501Y. V2B.1.351) has faced a rapid increase in COVID-19 mediated by new variants (*Dawood, 2020*; *Korber et al., 2020*). One way of recovering from this problem could be to identify potent COVID-19 inhibitors are urgently needed, as the situation getting worst. In this regard, plants serve as the source of therapeutic ingredients in the history of the human race. As far as we know, little previous research has investigated curcumin sp

polyphenols inhibitory effect on COVID-19. Curcumin consists of three major compounds, namely, diferuloylmethane (60–70%), demethoxycurcumin (20–27%), and Bisdemethoxycurcumin (10–15%) (*Heger et al., 2013*; *Nelson et al., 2017*). The review showed Curcumin-derived polyphenols exhibit antiviral activity for influenza, hepatitis C virus, HIV, anti-inflammatory, antibacterial, and antioxidant properties and also exert substantial anticarcinogenic activities (*Heger et al., 2013*; *Nelson et al., 2017*; *Praditya et al., 2019b*). Wet lab experimental approaches for the study of interactions between therapeutic substance and target proteins are not cheap, not safe, labors, and time-consuming (*Basak et al., 2020*; *Bachmann & Lewis, 2005*). There are many alternative methods are available for solving these problems. In this study, we proposed the combinational strategy of docking and molecular dynamics simulation. A series of recent studies have indicated that combinational strategy of the docking and molecular dynamic simulations techniques identify the targets for several bioactive compounds whose in vivo targets are unknown including COVID-19 (*Rahman et al., 2020*; *Fiesco-Sepúlveda & Serrano-Bermúdez, 2020*; *Cortés-García et al., 2020*). This study aims to investigate the binding affinity of three Curcumin-derived polyphenols against COVID-19 the main protease (Mpro) binding pocket (Mpro) and the identification of important residues for interaction with curcumin-derived polyphenols. For this purpose, we used protein-carmofur (PDB code: 7BUY) as a model to offer evidence that could elucidate the mechanisms of curcumin sp polyphenols inhibition. At the beginning of this study, curcumin sp-derived polyphenols were subjected to ADMETox evaluation. According to Proudfooti's rule states that for any compound to be selected as a potential drug it should have; molar refractivity between 40 and 130, Less than 10 hydrogen bond acceptors, less than 5 hydrogen bond donors, high lipophilicity (expressed as LogP ≤ 5) and Molecular mass <500 Dalton. Therefore, three selected curcumin sp-derived polyphenols used in this study passed all the five criteria mentioned in Proudfoot's rule (Table S3). Demethoxycurcumin and bisdemethoxycurcumin polyphenol passed the ADME evaluation and throughout the screening, only Diferuloylmethane passed the predicted toxicity evaluation. Thus this study suggests that these phytochemicals have the potential to work effectively as drugs. Next, to validate our docking methodology crystal structure of COVID-19 main protease binding pocket (Mpro) (PDB code: 7BUY) with carmofur bound at the binding pocket was retrieved from PDB and re-dock with carmofur. The values of the RMSD between the Mpro crystals structure (RMSD 1.6) and the re-dock structures (RMSD 1.9) confirmed a close-match between docked and original structures. This confirmed our model structure is good quality and continued docking our work. Molecular docking studies showed that curcumin polyphenols have binding energy values between −12.17 to −12.32 kcal/mol^{-1} as shown in Table 1. Recent theoretical developments have revealed that Docking studies on different traditional medicine inhibitors activity for the SARS-CoV-2 protease. Several studies have been reported the binding energy of molecules less than or/and higher values compared to this study. Cherrak et al. reported in the literature that Quercetin-3-O-rhamnoside showed the highest binding affinity −7kcal/mol^{-1} (*Cherrak, Merzouk & Mokhtari-Soulimane, 2020*). Moreover, it was observed that curcumin exhibited the highest binding free energy of −18.21 kcal/mol^{-1} in different COVID-19 main protease, which is targeted in this study (*Adeoye,*

Table 1 Molecular docking results to determine the SARS CoV-2 main protease (Mpro) binding pocket affinity towards selected curcumin sp derived polyphenols at 298.15 K.

Protein-ligand complexes	Binding energy (kcal/mol)	Inhibition constant (Ki) (uM)	RMSD[b] (A⁰)	Residues involved in interaction	No of hydrogen bonds
Diferuloylmethane-COVID-19 main protease	−12.25	156.42	70.645	Asn142 and Gln192	2
Demethoxycurcumin-COVID-19 main protease	−12.17	281.22	57.842	Leu272, Thr199,Lys137	3
Bisdemethoxycurcumin-COVID-19 main protease	−12.32	98.83	65.030	Phe294, Gln110 and Glu240	3

2020). And also, docking of SARS-CoV-2 spike protein (PDB ID: 6LU7) with nelfinavir, lopinavir, kaempferol, quercetin, luteolin-7-glucoside,demethoxycurcumin, naringenin, apigenin-7-glucoside, oleuropein, curcumin, catechin, epicatechin-gallate, gingerol, gingerol, and allicin binding energies ranges between −4.03 to −7.6 kcal/mol^{-1} (*Khaerunnisa et al., 2020*). Recently, Computational docking of 14 compounds representing flavonoids, phenolic acids, and terpenes from honey and propolis with two different targets from COVID-19 showed binding affinity ranges between −5.6 to −7.8 kcal/mol^{-1} (*Dawood, 2020*). Bisdemethoxycurcumin, Demethoxycurcumin, and Diferuloylmethane revealed a minimum of two hydrogen bonds and a maximum of three hydrogen bonds for the Mpro binding pocket of SARS-CoV-2 (Table 1). In line with previous studies, hydrogen bonds are the most important bonds in determining the binding affinity, selectivity, and stabilization effect of curcumin-derived polyphenols with Mpro (*Baby et al., 2020*). The inhibition constant (Ki) is higher for Demethoxycurcumin (281.22 uM) than Bisdemethoxycurcumin (98.83 uM) and Diferuloylmethane (156.42 uM) as shown in Table 1. Prior research suggests that the smaller the Ki, the greater the binding affinity and the smaller amount of medication needed to inhibit the activity of that enzyme (*Bachmann & Lewis, 2005*). The RMSD values obtained for the lowest-energy poses predicted for each polyphenol are shown in Table 1 and average RMSD results ranging from 57.0 to 70.0 Å RMSD. But this is not relevant data for this study.

Furthermore, residues forming stable contact with polyphenols include Phe294, Gln110, Gln240, Gln192 Asn142, Lys137, Thr199, and Leu272 with probabilities larger than 85% (Fig. 5, Table 1). Bisdemethoxycurcumin and Demethoxycurcumin have lost hydrophobic interaction with Pro293 with Tyr239, respectively (Fig. 1). Besides this, a total of eight residue pairs that have average distances smaller than 10.0 Å within free enzyme residues and Mpro-polyphenols complexes binding pocket residues and surface residues were reported (Table 2). This implies that residue from both surface and binding pocket protein is involved in direct contact with curcumin-derived polyphenols. Furthermore, the inter-residue distances between the binding pocket and surface residues in Mpro-bisdemethoxycurcumin and Mpro-demethoxycurcumin complex are slightly different from that of Mpro-diferuloylmethane, particularly for Pro252/Lys137, Thr292/Thr199, Ile200/Leu272, and Arg188/Phe294 residues (Table 2). In line with
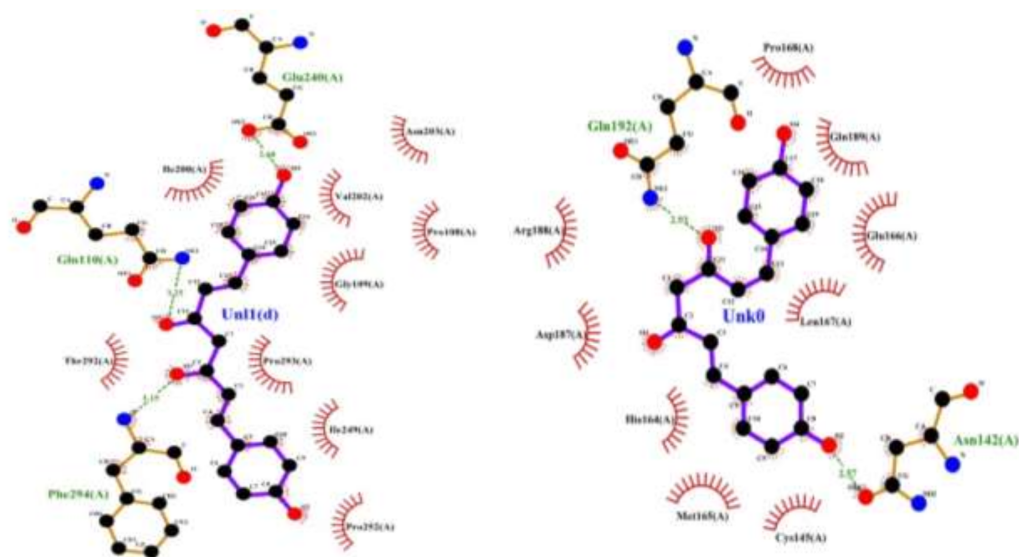
Bisdemethoxycurcumin- COVID-19 main protease

Diferuloylmethane -COVID-19 main protease
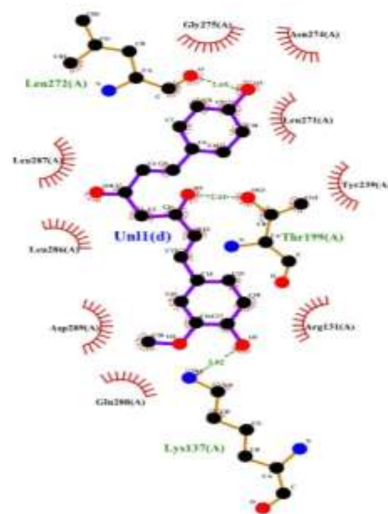
Demethoxycurcumin- COVID-19 main protease

Figure 1 Interactions of selected polyphenols and Main protease binding pocket residues. For all polyphenols, carbon atoms are shown in black, oxygens in red, and nitrogens in blue. Bonds in the Diferuloylmethane, Demethoxycurcumin, and Bisdemethoxycurcumin are shown in purple, and bonds in binding pocket residues are in brown. Hydrogen bonds are shown (with their lengths) as green dashed lines. Residues making hydrophobic interactions with the Diferuloylmethane, Demethoxycurcumin, and Bisdemethoxycurcumin are shown as red arcs with radiating lines. Diferuloylmethane, Demethoxycurcumin, and Bisdemethoxycurcumin atoms involved in these hydrophobic interactions are shown with radiating red lines. Full-size ⬜ DOI: 10.7717/peerj.11590/fig-1

previous studies, residue serine interacts with residue Phe140 and Glu166 to stabilize the enzyme- polyphenols complex binding site (*Jin et al., 2020*). For residues Gln192, Leu167, Ser144, Gly143, His114, Pro168, His41, and Cys145, their contact probabilities with

Table 2 Inter-residue distances and corresponding standard deviations. In each residue pair, one belongs to the binding pocket loop region and the other belongs to surface part of the enzyme.

Residues	Free enzyme	Enzyme-demethoxycurcumin complex	Enzyme-bisdemethoxycurcumin complex
Arg188–Phe294	5.154 ± 1.531	5.937 ± 1.604	4.5 ± 1.10
Val202–Gln110	9.419 ± 1.440	8.455 ± 1.090	9.25 ± 1.440
Gly109–Gln240	10.111 ± 1.838	8.296 ± 1.459	11.31 ± 1.14
Pro293–Gln192	8.570 ± 1.663	7.095 ± 1.022	5.13 ± 1.04
Ile249–Asn142	9.170 ± 5.015	10.485 ± 1.560	6.71 ± 0.44
Pro252–Lys137	7.11 ± 0.02	8.5 ± 1.4	5.63 ± 1.04
Thr292–Thr199	5.109 ± 0.440	6.039 ± 0.940	4.110 ± 0.230
Ile200–Leu272	7.213 ± 0.018	9.216 ± 0.218	6.121 ± 0.618
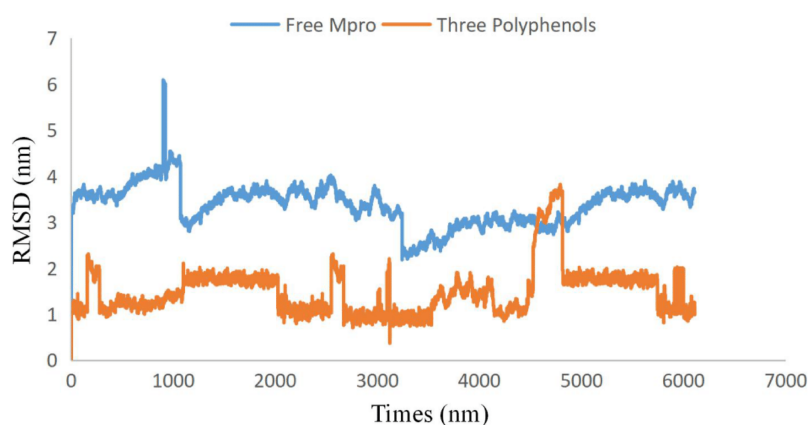
Figure 2 Plots of root-mean-square deviations of free SARS CoV-2 main protease (Mpro) (blue) and the complex of SARS CoV-2 main protease (7BUY) (red) with three polyphenols along the MD simulation time. Free SARS CoV-2 main protease (Mpro) (blue) and the complex of SARS CoV-2 main protease (7BUY) (red) with three polyphenols. Full-size ⬛ DOI: 10.7717/peerj.11590/fig-2

bisdemethoxycurcumin were increased significantly and Cys145 is a key catalytic residue which is consistent with a previous study (*Jin et al., 2020*). Residues forming stable contact with polyphenol include Phe294, Gln110, Gln240, Gln192 Asn142 Lys137 Thr199, and Leu272 the complexes with probabilities larger than 85% (Fig. 1). Also, for residues Glu288, Asp289, Leu287 Arg131, Tyr239, Leu271, Asn274, Gly275, and Leu286 the probabilities of contacts between demethoxycurcumin increased significantly after binding and they also form stable contacts (Fig. 2). For residues Arg188, Val202, Gly109, Pro293, Ile249, Pro252, Thr292, Ile200, and Cys145 their contact probabilities with bisdemethoxycurcumin were increased significantly and Cys145 is a key catalytic residue which is consistent with a previous study (*Jin et al., 2020*). Pro168, His41, and Val116 residues contact probabilities between demethoxycurcumin-Mpro and bisdemethoxycurcumin-Mpro decreased (Table 3). Previous studies have shown COVID-19 main protease possesses a dynamic binding pocket loop comprising domain-I (residues 10–99) and domain-II (residues

Table 3 Residues forming contacts with diferuloylmethane polyphenol, demethoxycurcumin polyphenol and bisdemethoxycurcumin polyphenol in binary complexes.

Residues	Enzyme-demethoxycurcumin complex	Enzyme bisdemethoxycurcumin complex	Enzyme-diferuloylmethane complex
Gln192	0.70 ± 0.01	0.85 ± 0.01	0.45 ± 0.02
Leu167	0.90 ± 0.03	0.98 ± 0.004	0.60 ± 0.05
Tyr239	0.60 ± 0..07	0.80 ± 0.01	0.30 ± 0.01
Asp289	0.70 ± 0.19	0.90 ± 0.004	0.60 ± 0.1
Arg188	0.75 ± 0.011	0.80 ± 0.05	0.73 ± 0.09
Glu166	0.80 ± 0.04	0.80 ± 0.01	0.90 ± 0.01
Glu288	1.00 ± 0.06	0.50 ± 0.01	0.60 ± 0.12
His114	1.00 ± 0.00	1.00 ± 0.00	0.50 ± 0.03
Gln189	0.70 ± 0.05	0.90 ± 0.00	1.00 ± 0.09
Pro168	0.30 ± 0.01	1.00 ± 0.00	0.85 ± 0.05
Gln189	0.45 ± 0.02	1.00 ± 0.00	0.40 ± 0.16
Cys145	0.75 ± 0.09	0.90 ± 0.01	0.60 ± 0.06
Met165	0.80 ± 0.1	0.85 ± 0.12	0.50. ± 0.12
His 164	0.40 ± 0.00	0.70 ± 0.01	1.00 ± 0.04
Asp187	0.90 ± 0.03	0.90 ± 0.03	0.90 ± 0.03
Arg188	0.93 ± 0.12	0.89 ± 0.01	0.76 ± 0.23
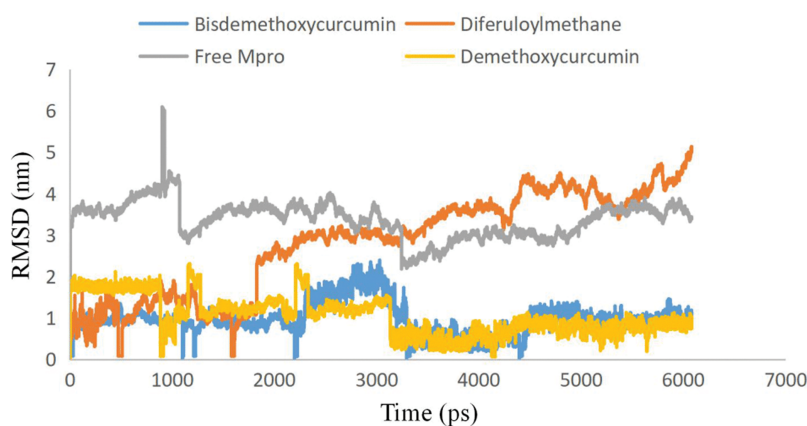
Figure 3 Plots of Root-mean-square deviations of free main CoV-2 protease (Mpro) (gray) and the complex of Mpro with Bisdemethoxycurcumin (yellow), Demethoxycurcumin (blue) and Diferuloylmethane (red) along the MD simulation time for three individual polyphenols. Free main CoV-2 protease (Mpro) (gray), the complex of Mpro with Bisdemethoxycurcumin (yellow), Demethoxycurcumin (blue) and Diferuloylmethane (red). Full-size ⬛ DOI: 10.7717/peerj.11590/fig-3

100–184), in which most of the residues in this study laid (*Jin et al., 2020*; *Kouznetsova et al., 2020*; *Kandeel, Kitade & Almubarak, 2020*).

To examine the stability and conformational dynamics of the Mpro–three curcumin-derived polyphenols complex and free Mpro, we calculated the RMSD for the backbones of all residues (Figs. 2 and 3). In this study, much attention has been given to the impact of curcumin derived polyphenols diferuloylmethane, demethoxycurcumin, and
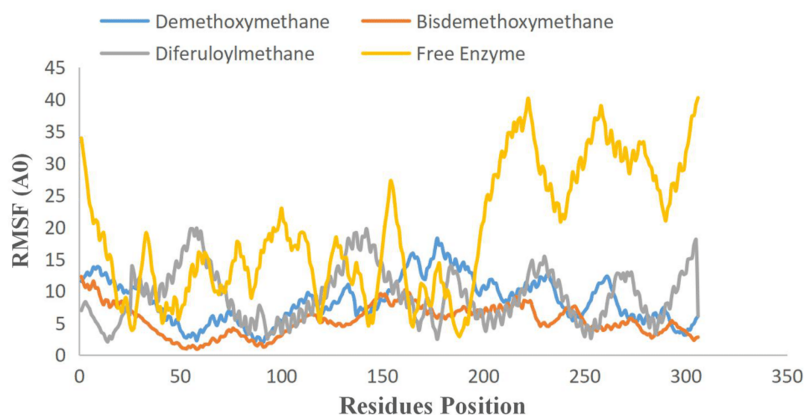
Figure 4 RMSF plot of free main CoV-2 protease (Mpro) (yellow) and the complex of Mpro with Bisdemethoxycurcumin (red), Demethoxycurcumin (blue) and Diferuloylmethane (gray) along the MD simulation time for three individual polyphenols. Free main CoV-2 protease (Mpro) (yellow), the complex of Mpro with Bisdemethoxycurcumin (red), Demethoxycurcumin (Blue) and Diferuloylmethane (gray). Full-size ◰ DOI: 10.7717/peerj.11590/fig-4

bisdemethoxycurcumin on the structure and dynamics of the main protease (Mpro). Here free Mpro has a significantly large root-mean-square deviation compare to curcumin sp polyphenols binding the Mpro pocket domain. The time evolution plot of RMSD displays the complex structure of diferuloylmethane- Mpro, demethoxycurcumin-Mpro, and bisdemethoxycurcumin-Mpro attain equilibrium at 1,000 ps and remains stable up to 5,000 ps (Fig. 2). In particular, the complex structure with demethoxycurcumin and bisdemethoxycurcumin is largely stabilized around 3,000–6,000 ps (Fig. 3). Likewise, its fluctuation main protease complex is smaller, especially in the segment Asn226–Gly252, which is the active-site loop region which is consistent with the previous study discussed (Fig. 4). Particularly, binding of the bisdemethoxycurcumin was observed to decrease RMSF of some segments (30–100, 200–250, and 250–300) and increase that of the segment (100–150) (Fig. 4). The higher value of RMSF depicted that the structure has some flexible regions while the lower value of RMSF indicated that the structure was good in terms of secondary structure (O'Boyle et al., 2011). Therefore, the result revealed the interactive stabilizing effect of Demethoxycurcumin and Bisdemethoxycurcumin. Also, the impact of these polyphenols on the structure and dynamics of the Main protease binding pocket domain region was further regulated by a hydrogen bond. Here, we also examine the time evolution of the hydrogen bond (H-bond) formed between the Mpro and curcumin sp derived polyphenols (Fig. 5). We found that the trajectory of bisdemethoxycurcumin revealed five H-bonds with Mpro, three H-bonds were seen consistently during the simulation (Fig. 5). Demethoxycurcumin revealed the presence of ten H-bonds with Mpro but, three H-bond can be seen retained throughout the simulation, the H-bond plot of diferuloylmethane shows a maximum of seven H-bond interactions with Mpro, but only two seen retained throughout the simulation (Fig. 5), while the carmofur showed a lesser number of hydrogen bonds (Jin et al., 2020). The strong hydrogen bonding interactions between the demethoxycurcumin-Mpro and bisdemethoxycurcumin-Mpro may be a potential inhibitor (Bolton et al., 2008). This study may contribute to the understanding of
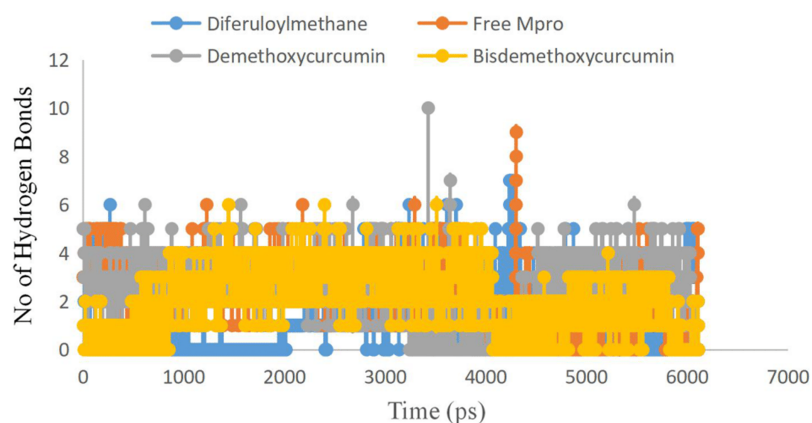
Figure 5 Number of hydrogen bond present in Bisdemethoxycurcumin-SARS-CoV-2 main protease (yellow), Demethoxycurcumin-SARS-CoV-2 main protease (gray), free SARS-CoV-2 main protease (red) and diferuloylmethane-main protease (blue). Bisdemethoxycurcumin-SARS-CoV-2 main protease (yellow), Demethoxycurcumin-SARS-CoV-2 main protease (gray), free SARS-CoV-2 main protease (red) and diferuloylmethane-main protease (blue). Full-size ▣ DOI: 10.7717/peerj.11590/fig-5

the structure-based design of COVID-19 therapy with curcumin-derived polyphenols. Future investigations are necessary to validate the kinds of conclusions that can be drawn from this study.

CONCLUSIONS

Until now, Great progress has been made in Computational methods involving drug target identification in a paradigm change in both industry and academics. Computational techniques, for example, data mining, homology modeling, MD simulation, cheminformatics, docking, and QSAR modeling have provided powerful techniques for target identification, drug discovery, and optimization. First, curcumin-derived polyphenols were subjected to in silico ADMETox and we found the potential ability to work effectively as drugs. Based on the results of the present study, it can be concluded that the investigated curcumin-derived polyphenols could interfere with the important residues in the enzymatic binding pocket to inhibit the main protease enzyme COVID-19 virus. Demethoxycurcumin and bisdemethoxycurcumin polyphenols are identified to have inhibitory activities against novel COVID-19 main protease. Bisdemethoxycurcumin has a stronger bond and high affinity with the Main protease (Mpro). Furthermore, the average RMSD values of the backbone atoms in docked curcumin sp derived polyphenols were calculated from 10,000 ps and showed stable RMSD values between 1 nm to 2 nm for Bisdemethoxycurcumin and Demethoxycurcumin at the reasonably consistent temperature (~300 K) and pressure (1 bar), whereas diferuloylmethane complex showed RMSD value between 5.5 and 6.2 with same cut-off parameters. These data validated that the docked Mpro-Bisdemethoxycurcumin complexes and Mpro-Demethoxycurcumin complexes are more stable than the Mpro-diferuloylmethane complex. To completely investigate the effects of curcumin-derived polyphenols, this study recommended the roles of polyphenols identified for further exploration in a wet lab experiment.

ACKNOWLEDGEMENTS

ADDITIONAL INFORMATION AND DECLARATIONS

Author Contributions
- Aweke Mulu conceived and designed the experiments, performed the experiments, analyzed the data, prepared figures and/or tables, authored or reviewed drafts of the paper, ran auto-dock and NAMD simulation on his computational lab, and approved the final draft.
- Mulugeta Gajaa analyzed the data, prepared figures and/or tables, authored or reviewed drafts of the paper, and approved the final draft.
- Haregewoin Bezu Woldekidan analyzed the data, authored or reviewed drafts of the paper, and approved the final draft.
- Jerusalem Fekadu W/mariam analyzed the data, prepared figures and/or tables, authored or reviewed drafts of the paper, and approved the final draft.

Data Availability
The following information was supplied regarding data availability:
Raw data is available in the Supplemental Files.

Supplemental Information
Supplemental information for this article can be found online at http://dx.doi.org/10.7717/peerj.11590#supplemental-information.

REFERENCES

Adeoye A. 2020. Pharmacoinformatics and hypothetical studies on allicin, curcumin, and gingerol as potential candidates against COVID-19-associated proteases. *Journal of Biomolecular Structure and Dynamics* **10(10)**:1–12 DOI 10.1080/07391102.2020.1813630.

Anandakrishnan R, Aguilar B, Onufriev AV. 2012. H++ 3.0: automating pK prediction and the preparation of biomolecular structures for atomistic molecular modeling and simulation. *Nucleic Acids Research* **4(W1)**:537–541 DOI 10.1093/nar/gks375.

Anbarasu K, Jayanthi S. 2018. Identification of curcumin derivatives as human LMTK3 inhibitors for breast cancer: a docking, dynamics, and MM/PBSA approach. *3 Biotech* **8(5)**:228–239 DOI 10.1007/s13205-018-1239-6.

Baby K, Maity S, Mehta CH, Suresh A, Nayak UY, Nayak Y. 2020. Targeting SARS-CoV-2 main protease: a computational drug repurposing study. *Archives of Medical Research* **52(1)**:38–47 DOI 10.1016/j.arcmed.2020.09.013.

Bachmann KA, Lewis JD. 2005. Predicting inhibitory drug-drug interactions and evaluating drug interaction reports using inhibition constants. *Annals of Pharmacotherapy* **39**:1064–1072.

Baell JB, Holloway GA. 2012. New substructure filters for removal of pan assay interference compounds (PAINS) from screening libraries and for their exclusion in bioassays. *Journal of Medicinal Chemistry* **53(7)**:2719–2740 DOI 10.1021/jm901137j.

Basak N, Girish GV, De Subrata K, Maiti S, SARBASHRI BANK. 2020. In-silico analysis of potential interaction of drugs and the SARS-CoV-2 spike protein. Epub ahead of print 21 May 2020. *Research Square* DOI 10.21203/rs.3.rs-30401/v1.

Benkert P, Künzli M, Schwede T. 2009. QMEAN server for protein model quality estimation. *Nucleic Acids Research* **37(Suppl. 2)**:510–514 DOI 10.1093/nar/gkp322.

Bolton EE, Wang Y, Thiessen PA, Bryant SH. 2008. PubChem: integrated platform of small molecules and biological activities. *Annual Reports in Computational Chemistry* **4(2008)**:217–241 DOI 10.1016/S1574-1400(08)00012-1.

Chen Y, Liu Q, Guo D. 2020. Emerging coronaviruses genome structure, replication and pathogenesis. *Journal of Medical Virology* **92(10)**:2249 DOI 10.1002/jmv.26234.

Cherrak SA, Merzouk H, Mokhtari-Soulimane N. 2020. Potential bioactive glycosylated flavonoids as SARS-CoV-2 main protease inhibitors: a molecular docking and simulation studies. *PLOS ONE* **15(10)**:e0240653 DOI 10.1371/journal.pone.0240653.

Colovos C, Yeates TO. 1993. Verification of protein structures: patterns of nonbonded atomic interactions. *Protein Science* **2(9)**:1511–1519 DOI 10.1002/pro.5560020916.

Cortés-García CJ, Chacón-García L, Mejía-Benavides JE, Díaz-Cervantes E. 2020. Tackling the SARS-CoV-2 main protease using hybrid derivatives of 1, 5-disubstituted tetrazole-1, 2, 3-triazoles: an in silico assay. *PeerJ Physical Chemistry* **2(2)**:e10 DOI 10.7717/peerj-pchem.10.

Daina A, Michielin O, Zoete V. 2017. SwissADME: a free web tool to evaluate pharmacokinetics, drug-likeness and medicinal chemistry friendliness of small molecules. *Scientific Reports* **7(1)**:42717 DOI 10.1038/srep42717.

Dash R, Bin Emran T, Nasir Uddin MM, Islam A, Junaid M. 2014. Molecular docking of fisetin with AD associated AChE, ABAD and BACE1 proteins. *Bioinformation* **10(9)**:562–568 DOI 10.6026/97320630010562.

Dawood AA. 2020. Mutated COVID-19 may foretell a great risk for mankind in the future. *New Microbes and New Infections* **35**:100673 DOI 10.1016/j.nmni.2020.100673.

Elaswad A, Fawzy M, Basiouni S, Shehata A. 2020. Mutational spectra of SARS-CoV-2 isolated from animals. *PeerJ* **8(7)**:e10609 DOI 10.7717/peerj.10609.

Emran TB, Rahman MA, Uddin MMN, Dash R, Hossen MF, Mohiuddin M, Alam MR. 2015. Molecular docking and inhibition studies on the interactions of Bacopa monnieri's potent phytochemicals against pathogenic Staphylococcus aureus. *DARU Journal of Pharmaceutical Sciences* **23(1)**:1–8 DOI 10.1186/s40199-015-0106-9.

Fiesco-Sepúlveda KY, Serrano-Bermúdez LM. 2020. Contributions of Latin American researchers in the understanding of the novel coronavirus outbreak: a literature review. *PeerJ* **8(4)**:e9332 DOI 10.7717/peerj.9332.

Forni C, Facchiano F, Bartoli M, Pieretti S, Facchiano A, D'Arcangelo D, Norelli S, Valle G, Nisini R, Beninati S, Tabolacci C, Jadeja RN. 2019. Beneficial role of phytochemicals on oxidative stress and age-related diseases. *BioMed Research International* **2019**:8748253 DOI 10.1155/2019/8748253.

Guarner J. 2020. Three emerging coronaviruses in two decades: the story of SARS, MERS, and now COVID-19. *American Journal of Clinical Pathology* **153(4)**:420–421 DOI 10.1093/ajcp/aqaa029.

Hatcher H, Planalp R, Cho J, Torti FM, Torti SV. 2008. Curcumin: from ancient medicine to current clinical trials. *Cellular and Molecular Life Sciences* **65(11)**:1631–1652 DOI 10.1007/s00018-008-7452-4.

Heger M, Van Golen RF, Broekgaarden M, Michel MC. 2013. The molecular basis for the pharmacokinetics and pharmacodynamics of curcumin and its metabolites in relation to cancer. *Pharmacological Reviews* **66(1)**:222–307 DOI 10.1124/pr.110.004044.

Hoque MN, Chaudhury A, Akanda MAM, Hossain MA, Islam MT. 2020. Genomic diversity and evolution, diagnosis, prevention, and therapeutics of the pandemic COVID-19 disease. *PeerJ* **8(3)**:e9689 DOI 10.7717/peerj.9689.

Islam MT, Khan MR, Mishra SK. 2019. An updated literature-based review: phytochemistry, pharmacology and therapeutic promises of *Nigella sativa* L. *Oriental Pharmacy and Experimental Medicine* **19(2)**:115 DOI 10.1007/s13596-019-00363-3.

Jin Z, Zhao Y, Sun Y, Zhang B, Wang H, Wu Y, Zhu Y, Zhu C, Hu T, Du X, Duan Y, Yu J, Yang X, Yang X, Yang K, Liu X, Guddat LW, Xiao G, Zhang L, Yang H, Rao Z. 2020. Structural basis for the inhibition of SARS-CoV-2 main protease by antineoplastic drug Carmofur. *Nature Structural and Molecular Biology* **27**:529–532.

Kandeel M, Kitade Y, Almubarak A. 2020. Repurposing FDA-approved phytomedicines, natural products, antivirals and cell protectives against SARS-CoV-2 RNA-dependent RNA-polymerase. *PeerJ* **8(14)**:e10480 DOI 10.7717/peerj.10480.

Khaerunnisa S, Kurniawan H, Awaluddin R, Suhartati S, Soetjipto S. 2020. Potential inhibitor of COVID-19 main protease (Mpro) from several medicinal plant compounds by molecular docking study. *Hindawi* **2020**:6307457 DOI 10.1155/2020/6307457.

Korber B, Fischer WM, Gnanakaran S, Yoon H, Theiler J, Abfalterer W, Hengartner N, Giorgi EE, Bhattacharya T, Foley B, Hastie KM, Parker MD, Partridge DG, Evans CM, Freeman TM, De Silva TI. 2020. Tracking changes in SARS-CoV-2 spike: evidence that D614G increases infectivity of the COVID-19 virus. *Cell* **182**:812–827.e19.

Kouznetsova VL, Zhang A, Tatineni M, Miller MA, Tsigelny IF. 2020. Potential COVID-19 papain-like protease PL[pro] inhibitors: repurposing FDA-approved drugs. *PeerJ* **8(1)**:e9965 DOI 10.7717/peerj.9965.

Kumari R, Kumari R, Lynn A. 2014. g_mmpbsa—a GROMACS tool for high throughput MM-PBSA calculations. *Journal of Chemical Information and Modeling* **54(7)**:1951–1962 DOI 10.1021/ci500020m.

Liu X, Zhang B, Jin Z, Yang H, Rao Z. 2020. The crystal structure of COVID-19 Main protease in complex with an inhibitor N3. *Journal of Chemical Information and Modeling* **60(7)**:3593–3602 DOI 10.1021/acs.jcim.0c00283.

Morris GM, Huey R, Lindstrom W, Sanner MF, Belew RK, Goodsell DS, Olson AJ. 2009. AutoDock4 and AutoDockTools4: automated docking with selective receptor flexibility. *Journal of Computational Chemistry* **30(16)**:2785–2791 DOI 10.1002/jcc.21256.

Mounce BC, Cesaro T, Carrau L, Vallet T, Vignuzzi M. 2017. Curcumin inhibits Zika and chikungunya virus infection by inhibiting cell binding. *Antiviral Research* **142**:148–157 DOI 10.1016/j.antiviral.2017.03.014.

Muralidharan N, Sakthivel R, Velmurugan D, Gromiha MM. 2020. Computational studies of drug repurposing and synergism of lopinavir, oseltamivir and ritonavir binding with SARS-CoV-2 protease against COVID-19. *Journal of Biomolecular Structure and Dynamics* **16(7)**:1–6 DOI 10.1080/07391102.2020.1752802.

Nelson KM, Dahlin JL, Bisson J, Graham J, Pauli GF, Walters MA. 2017. The essential medicinal chemistry of curcumin. *Journal of Medicinal Chemistry* **60(5)**:1620–1637 DOI 10.1021/acs.jmedchem.6b00975.

Nelson M, Humphrey W, Gursoy A, Dalke A, Kalé LV, Skeel RD, Schulten K. 1996. NAMD—a parallel, object-oriented molecular dynamics program. *International Journal of Supercomputer Applications and High Performance Computing* **10(4)**:251–268 DOI 10.1177/109434209601000401.

O'Boyle NM, Banck M, James CA, Morley C, Vandermeersch T, Hutchison GR. 2011. Open babel: an open chemical toolbox. *Journal of Cheminformatics* **3(1)**:33 DOI 10.1186/1758-2946-3-33.

Pal M, Berhanu G, Desalegn C, Kandi V. 2020. Severe acute respiratory syndrome coronavirus-2 (SARS-CoV-2): an update. *Cureus* **12(3)**:e7423 DOI 10.7759/cureus.7423.

Parlikar A, Kalia K, Sinha S, Patnaik S, Sharma N, Vemuri SG, Sharma G. 2020. Understanding genomic diversity, pan-genome, and evolution of SARS-CoV-2. *PeerJ* **8(3)**:e9576 DOI 10.7717/peerj.9576.

Pontius J, Richelle J, Wodak SJ. 1996. Deviations from standard atomic volumes as a quality measure for protein crystal structures. *Journal of Molecular Biology* **264(1)**:121–136 DOI 10.1006/jmbi.1996.0628.

Praditya D, Kirchhoff L, Bruning J, Rachmawati H, Steinmann J, Steinmann E. 2019a. Anti-infective properties of the golden spice curcumin. *Frontiers in Microbiology* **10**:912 DOI 10.3389/fmicb.2019.00912.

Praditya D, Kirchhoff L, Brüning J, Rachmawati H, Steinmannand J, Steinmann E. 2019b. Anti-infective properties of the golden spice curcumin. *Frontiers in Microbiology* **10**:912 DOI 10.3389/fmicb.2019.00912.

Rahman MS, Hoque MN, Islam MR, Akter S, Rubayet U, Alam ASM, Siddique MA, Saha O, Rahaman MM, Sultana M, Crandall KA, Hossain MA. 2020. Epitope-based chimeric peptide vaccine design against S, M and E proteins of SARS-CoV-2 etiologic agent of global pandemic COVID-19: an in silico approach. *PeerJ* **8(2)**:e9572 DOI 10.7717/peerj.9572.

Vanommeslaeghe K, Raman EP, MacKerell AD. 2012. Automation of the CHARMM General Force Field (CGenFF) II: assignment of bonded parameters and partial atomic charges. *Journal of Chemical Information and Modeling* **52(12)**:3155–3168 DOI 10.1021/ci3003649.

WHO. 2020. *Director-general's opening remarks at the media briefing on COVID-19—3 March 2020*. Geneva: World Health Organization.

Woo PCY, Huang Y, Lau SKP, Yuen KY. 2010. Coronavirus genomics and bioinformatics analysis. *Viruses* **2(8)**:1804–1820 DOI 10.3390/v2081803.

World Health Organization. 2020. Coronavirus disease 2019 (COVID-19) situation report—43. *Available at https://www.who.int/emergencies/diseases/novel-coronavirus-2019/situation-reports*.

Zhao Q, Weber E, Yang H. 2013. Recent developments on coronavirus main protease/3C like protease inhibitors. *Recent Patents on Anti-Infective Drug Discovery* **8(2)**:150–156 DOI 10.2174/1574891X113089990017.